Journal of Structural Geology, Vol. 10, No. 2, pp. 211 to 218, 1988
Printed in Great Britain

0191-8141/88 $03.00 + 0.00

The geometrical significance of strain trajectory curvature

P. R. COBBOLD and E. BARBOTIN

Centre Armoricain d'Etude Structurale des Socles (CNRS), Université de Rennes, 35042 Rennes Cédex, France

(*Received* 20 *December* 1986; *accepted in revised form* 12 *November* 1987)

Abstract—We derive the following two-dimensional equations for the curvature of intersecting strain trajectories:

$$K_1 = \lambda_2(k_1 - f_1); \quad K_2 = \lambda_1(k_2 - f_2).$$

The subscripts refer to one or the other trajectory; K expresses curvature in the undeformed state; k, curvature in deformed state; λ is the stretch (final length divided by original length); and f is the flexure, a logarithmic strain gradient defined for each trajectory as $f_1 = -\partial\varepsilon_1/\partial s_2$ and $f_2 = \partial\varepsilon_2/\partial s_1$, where $\varepsilon = \ln\lambda$ is logarithmic stretch and s is true arc length along a trajectory. The curvature equations are simple forms of the equations of strain compatibility. We derive them from first principles in the Appendix.

In the main text, we illustrate and verify the curvature equations using six theoretical examples of strain fields and an experimental one. Each theoretical example is deliberately chosen to illustrate the contribution of one or more terms in the curvature equations. The first four examples are single fans, where trajectories are polar co-ordinates. The other three examples are double fans from more complex strain fields.

The equations and examples sometimes uphold and sometimes contradict the convergence hypothesis, in which strain intensity is assumed to increase as trajectories converge. The equations also show that strain gradients can exist even if both trajectories have no curvature and there are no volume changes. In practice, if a geologist knows only the trajectory curvatures at one point in the deformed state, he cannot determine strain gradients, because there are too many unknowns in the curvature equations.

INTRODUCTION

IN THE last two decades, detailed measurements have been made in ductile rocks at various scales throughout tectonic regions. Such studies have shown that strain is commonly non-uniform across a given region. One of the challenges of structural geology is to obtain good strain data and so to establish strain patterns with confidence. Other more mathematical challenges are to interpret strain patterns geometrically and to develop reliable methods for reversing the strains and obtaining tectonic displacements (Schwerdtner 1977, Cobbold 1977, 1979, 1980, Cobbold & Percevault 1983).

Where strain data are sparse, it may be helpful to know that strain components cannot vary independently of one another in space: they must satisfy compatibility equations. These equations can be expressed in terms of principal directions and principal values. In some regions, principal directions of strain are more readily obtained than principal values. This is especially so if there is a cleavage or a stretch lineation that tracks a principal direction of strain to within a few degrees or so (Ramsay 1967, Siddans 1972, Wood 1974). Cleavage or lineation trajectories can then be drawn and may closely approximate strain trajectories, although such an interpretation is questionable in some instances (Williams 1976). Once strain trajectories are obtained, what constraints do the equations of strain compatibility put upon strain values?

Where strain is non-uniform, strain trajectories are often (but not necessarily) curved. Cleavage trajectories and lineation trajectories are commonly curved in natural rocks, good examples being sigmoidal cleavage patterns across shear zones (Ramsay & Graham 1970). Where one trajectory is curved, the set normal to it forms a fan. Convergent (or divergent) cleavage fans are common features of folds (Ramsay 1967) and they suggest non-uniform strain.

Thus it seems appropriate to study the geometrical significance of trajectory curvature and convergence. One question of interest is the possible correlation between a convergence of trajectories and an increase in strain intensity. Such a correlation seems to occur in many natural shear zones and folds (Ramsay 1967, Ramsay & Graham 1970). It has also been demonstrated to occur in some theoretical examples of strain patterns (Ramsay & Huber 1983, p. 43). Hence it has led to the following assertions.

(1) "Slaty cleavage planes converge toward the region of highest strain" (Ramsay 1967, p. 181).

(2) "A special geometric feature of strain trajectories is that they converge or diverge. In fact, if they are parallel it means either that the strain is homogeneous or that they coincide with special types of area change. Apart from these special cases, the e_1 trajectories always converge as we pass from a region of low strain into a region of high strain, whereas the e_2 trajectories diverge as we pass from low to high strains" (Ramsay & Huber 1983, p. 42).

(3) "It follows that cleavage planes represent the traces of the XY planes of adjacent strain ellipsoids and that cleavage must obey the geometric rules of finite strain trajectories. In our investigations of two-dimensional heterogeneous strain we concluded that the con-

vergence or divergence of X-finite strain trajectories went together with increase and decrease in finite strain values, respectively. The same holds true for three-dimensional XY finite strain trajectories and cleavage planes. Where cleavage planes converge, the finite strain X/Z ratios increase and this convergence goes together with an increase in the intensity of the cleavage" (Ramsay & Huber 1983, p. 184).

These assertions are forms of what we call the convergence hypothesis, defined precisely later on. To our knowledge, this hypothesis has never been investigated in a general way. We feel this has become all the more necessary, now that the hypothesis has been shown to break down for certain theoretical strain patterns within folds (Ramsay & Huber 1987, p. 457).

In this paper, we investigate the geometrical significance of strain trajectory curvature. We use the general theory of non-uniform strain in two dimensions to derive the curvature equations for trajectories (see Appendix). These are special forms of the compatibility equations previously derived in a geological context by Cobbold (1977, 1980) and reviewed by Cutler & Cobbold (1985). For conformity with these papers, we once again follow (as much as possible) the terminology of Truesdell & Toupin (1960), including the use of λ for stretch (final length divided by original length).

In the main text, we illustrate and verify the curvature equations using simple theoretical strain patterns and one experimental one. Each theoretical pattern has been specially chosen to illustrate the contribution of one or another term in the curvature equations. Hence the patterns are not all geologically realistic. They do show, however, why the convergence hypothesis holds in some situations, but not in others, and this is their main value.

CURVATURE EQUATIONS IN 2-D

Consider a set of principal strain trajectories in the deformed state (Fig. 1b). For convenience we use a grid of orthogonal curvilinear co-ordinates, x_1 and x_2, which coincide with the trajectories and are thus called principal co-ordinates. Similarly we use another grid of principal co-ordinates, X_1 and X_2, to describe strain trajectories in the undeformed state; in other words, trajectories for reciprocal strain ellipses (Fig. 1a). To compare the two grids, we refer them to a common Cartesian frame, labelled z_1, z_2 in the deformed state, and Z_1, Z_2 in the undeformed state, such that α is the angle between x_1 and z_1 (Fig. A1) and A, the angle between X_1 and Z_1 (see Truesdell & Toupin 1960, Cobbold 1980). At a given material point, trajectories in the deformed state have curvatures which we measure using the parameters $k_1 = \partial\alpha/\partial s_1$, and $k_2 = \partial\alpha/\partial s_2$, where s_1 and s_2 are true arc lengths along x_1 and x_2; similarly, in the undeformed state, $K_1 = \partial A/\partial S_1$ and $K_2 = \partial A/\partial S_2$, where S_1 and S_2 are arc lengths along X_1 and X_2.

True curvatures are, by convention, positive quantities (see Appendix). Our measures are curvatures, but with signs attached (positive or negative, to distinguish concave from convex curves, as in Fig. A1).We call these quantities directional curvatures.

As a result of deformation, a material line lying under X_1 (strain trajectory in the undeformed state) comes to lie under x_1 (strain trajectory in the deformed state), as discussed in more detail by Cobbold (1979). Although not strictly necessary, it is mathematically convenient and by no means restrictive to define the co-ordinates so that $x_1 = X_1$ and $x_2 = X_2$ (Cobbold 1980). This leads to a simple relationship between the directional curvatures (see Appendix):

$$K_1 = \lambda_2(k_1 - f_1) \tag{1a}$$

$$K_2 = \lambda_1(k_2 - f_2), \tag{1b}$$

where λ_1 and λ_2 are principal stretches along x_1 and x_2, respectively, and where f_1 and f_2 are strain gradients of the kind we call *flexures* and are defined as

$$f_1 = -\partial\varepsilon_1/\partial s_2; \quad f_2 = \partial\varepsilon_2/\partial s_1. \tag{2}$$

Here, $\varepsilon_1 = \ln\lambda_1$ and $\varepsilon_2 = \ln\lambda_2$ are logarithmic stretches.

Each curvature equation, for example (1a), indicates that the initial curvature (K_1) can be calculated, knowing: (i) the final curvature (k_1); (ii) the transverse stretch (λ_2); and (iii) the flexure (f_1) or transverse gradient of trajectory-parallel stretch. Throughout a general strain field, each of these parameters is liable to vary.

We now illustrate and verify the curvature equations for four specific examples of ideal single trajectory fans. At the same time, we discuss the geometric characteristics of these examples and test the convergence hypothesis. The examples are so chosen that one or other parameter, in the curvature equations, vanishes. Thus we illustrate the separate contribution of each parameter to trajectory curvature.

IDEAL SINGLE FANS

In the following ideal single fans, trajectories of one family are radiating straight lines, whereas trajectories of the other family are concentric circular arcs. Thus the principal co-ordinates used to describe them are, in fact, polar co-ordinates. For simplicity, we assume that values of stretch can vary along radii, but not along arcs of circles. This means that radiating straight lines in the deformed state were also straight lines (radiating or parallel) in the undeformed state. One of the two curvature equations thus vanishes totally and we need consider only the other equation.

Example 1 (*Fig.* 1). *Simple flexure*

In this example, trajectories of each family are assumed to be parallel straight lines in the undeformed state, so that $K_1 = K_2 = 0$ (Fig. 1a). At later stages

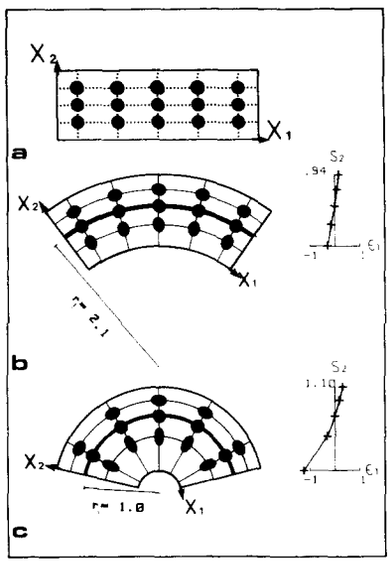

Fig. 1. Simple flexure. Configurations of material lines and objects (black) are shown in undeformed state (a) and two stages of deformation (b and c). In the deformed state (b and c), orthogonal curvilinear co-ordinates (x_1, x_2) are taken parallel to strain trajectories. In the undeformed state (a), orthogonal curvilinear co-ordinates (X_1, X_2) are taken tangent to principal directions of the reciprocal strain ellipse. They happen to be cartesian in this example (dotted lines). As a result of deformation, material lines initially lying parallel to X_1 or X_2 come to lie parallel to x_1 or x_2 (Cobbold 1979). In this example, one curved trajectory of the x_1 family (thick line) maintains its length; its radius of curvature (r_1) decreases from a value of 2.1 to a value of 1.0 length units. Profiles (right) show logarithmic stretch (ε_1) of x_1 trajectories as a function of true radial distance (s_2).

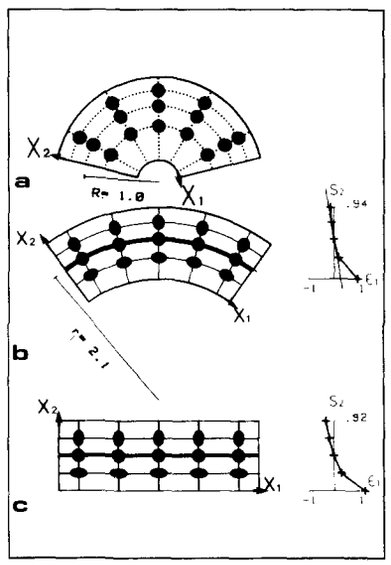

Fig. 2. Inverse flexure. For legend, see Fig. 1. For explanation, see text.

(Fig. 1b & c), one family (x_1 lines) becomes increasingly curved, whereas the other family (x_2 lines) diverges. Strain increments accumulate coaxially. The example has been drawn with no dilations (area changes). We focus attention on one trajectory that maintains a steady length (thick line, Fig. 1). Anywhere along this line, $\lambda_1 = \lambda_2 = 1$ and the curvature equation (1a) reduces to:

$$k_1 = f_1 = -\partial\varepsilon_1/\partial s_2. \tag{3}$$

Equation (3) states that the directional curvature is equal to the flexure. It can be verified graphically, using profiles of logarithmic stretch (Fig. 1b & c). At the unextended trajectory, the profile gradient, $-1/2.1$ reciprocal length units (r.l.u.) in Fig. 1(b), -1 r.l.u. in Fig. 1(c), is equal to k_1. The radius of curvature, r_1, is the reciprocal of the true curvature, which is the absolute value of k_1.

Both equation (3) and a casual inspection show that, throughout Fig. 1, as x_2 lines converge, λ_1 values decrease. To ensure no volume change, λ_2 values increase. Below the unextended line, this means that λ_{max} values and strain intensity both increase, as λ_{max} trajectories converge. In contrast, above the unextended line, λ_{max} values decrease as λ_{min} trajectories converge. Clearly it is more general to refer to λ_1, λ_2, x_1 and x_2, rather than to decide which is λ_{max} and which is λ_{min}. We bear this distinction in mind during tests of the convergence hypothesis, which we restate as follows: λ_1 values decrease as x_2 lines converge. Thus, in this example, the convergence hypothesis holds.

Example 2 (*Fig.* 2). *Inverse flexure*

The deformation here is mathematically the inverse of that in example 1. Trajectories of one family are curved in the undeformed state (Fig. 2a), but the curvature decreases with deformation (Fig. 2b), until it vanishes and the trajectories become straight lines (Fig. 2c). As before, strain increments accumulate coaxially and there are no dilations. We focus attention once again on a line that undergoes no length change (thick line, Fig. 2), so that $\lambda_1 = \lambda_2 = 1$. In the final deformed state (Fig. 2c), $k_1 = k_2 = 0$ and the curvature equation (1a) therefore reduces to:

$$K_1 = -f_1 = \partial\varepsilon_1/\partial s_2. \tag{4}$$

This equation is similar to equation (3), valid for example 1, except for the positive sign on the right-hand side and the capital letters on the left (referring to curvature in the undeformed state). This example shows that trajectories in the deformed state can be straight lines, even if there is a strain gradient and no dilation (cf. Ramsay & Huber 1983, p. 42). The result can be verified numerically, using a logarithmic stretch profile (Fig. 2c). This yields a gradient of -1 r.l.u., the negative reciprocal of the radius of curvature R_1 in the undeformed state. Because there is a stretch gradient but no curvature in the final deformed state, the convergence hypothesis breaks down.

For the intermediate deformed state (Fig. 2b), the curvature equation for the unextended line reduces to:

$$K_1 = k_1 - f_1, \tag{5}$$

meaning that the trajectory has non-zero curvatures in both the deformed and undeformed states. The difference between the directional curvatures is the flexure, f_1. Because this has a positive value, $K_1 < k_1$. We see that λ_1 values increase as x_2 trajectories converge. Thus the convergence hypothesis is not valid in this example.

The reader may wonder if this example is geologically

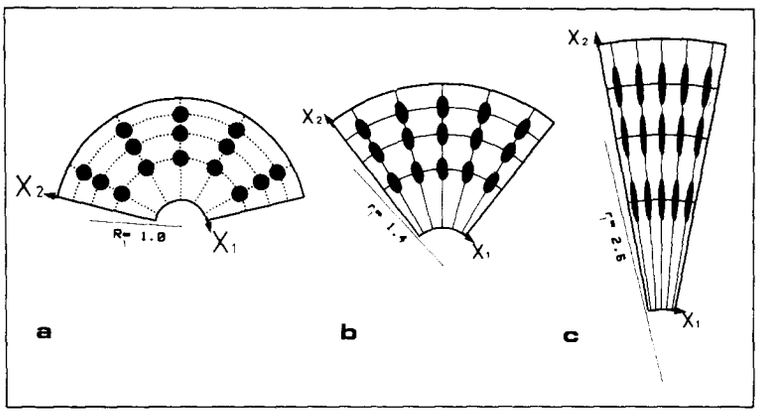

Fig. 3. Uniform radial stretch. For legend, see Fig. 1. For explanation, see text.

relevant, even though it is kinematically admissible. One possible application is to the straightening of an originally curved layer, for example a channel infill. Such an occurrence may be rare, but it is by no means impossible. Later we will give another application which may be geologically more common.

Example 3 (*Fig.* 3). *Uniform radial stretch*

Trajectory curvature can decrease, not only by inverse flexure (Fig. 2), but also if all radii of curvature stretch by a common factor, λ_2. The resulting pattern of uniform radial stretch (Fig. 3) can be achieved without dilation, all arcs suffering equal stretches of $\lambda_1 = 1/\lambda_2$. Thus flexures are non-existant ($f_1 = f_2 = 0$) and the curvature equation reduces to:

$$K_1 = \lambda_2 k_1. \tag{6}$$

This simply states that the radius of curvature stretches by a factor λ_2 during deformation. As λ_2 attains large values, so the curvature falls to zero (Fig. 3c).

Because the x_2 trajectories converge but there are no strain gradients, the convergence hypothesis does not hold in this example.

A uniform radial stretch is relevant to the buckling of embedded layers, but in general it occurs together with some flexure, as in the following example.

Example 4 (*Fig.* 4). *Flexure combined with radial stretch*

The previous examples of flexure (Fig. 1) or inverse flexure (Fig. 2), can be combined in any sequence or proportion with uniform radial stretch (Fig. 3). We show a special combination such that the directional curvature of one trajectory (thick line, Fig. 4d) does not change. Thus a first increment of uniform radial stretch results in an increase in radius of curvature (Fig. 4b); but the original curvature can be restored (Fig. 4d) by an increment of flexure. Alternatively, a first increment of flexure (Fig. 4c) may be followed by an increment of radial stretch, to yield the same result. For this special example, $k_1 = K_1$ and the curvature equation reduces to:

$$K_1 = k_1 = -f_1\lambda_2/(1 - \lambda_2), \tag{7}$$

which shows how f_1 and λ_2 can vary together to maintain a given directional curvature.

Finally, for this example, the convergence hypothesis holds (Fig. 4d).

Summary so far

In general, for a single fan, the curvature equation cannot be reduced, so that final directional curvature depends upon: (i) initial curvature; (ii) radial stretch; and (iii) radial gradient of arc-parallel stretch. The separate and combined effects of each of these parameters have been illustrated and verified in the previous examples. The convergence hypothesis holds in some examples, but not in others, depending upon the relative values and signs of the parameters in the curvature equation.

DOUBLE FANS IN GENERAL STRAIN FIELDS

At a typical point in a general 2-D strain field, both intersecting strain trajectories have curvature. This means that adjacent (closely spaced) trajectories of

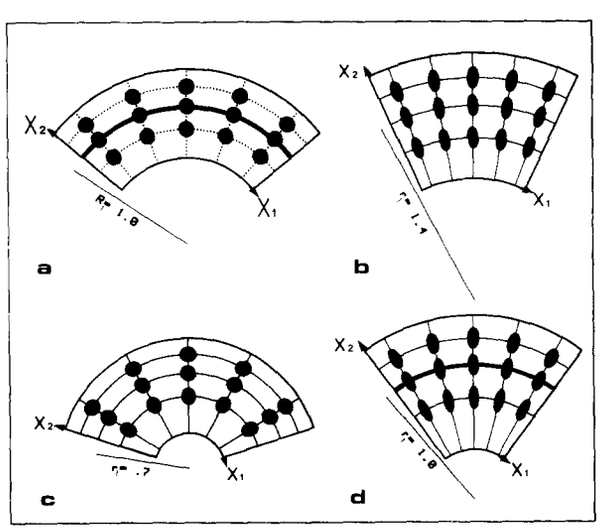

Fig. 4. Flexure combined with radial stretch. For legend, see Fig. 1. For explanation, see text.

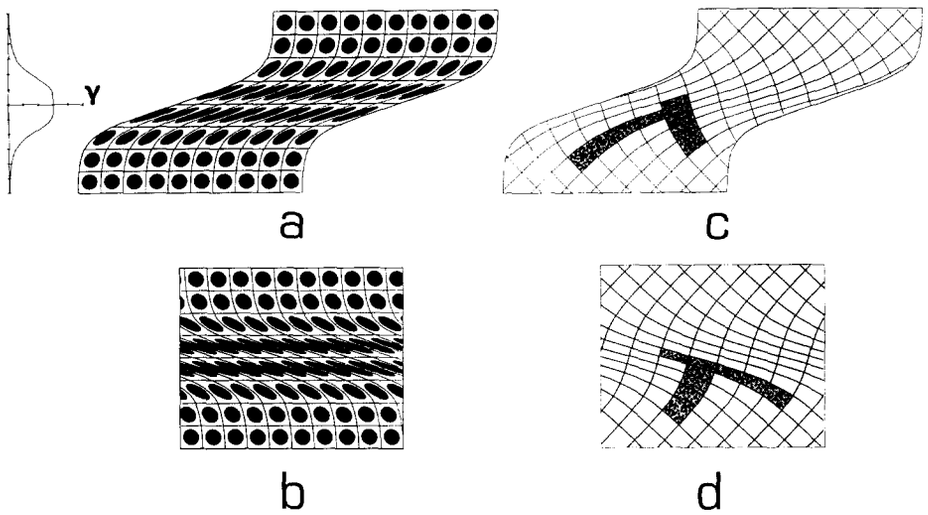

Fig. 5. Shear zone. Deformed state (a) shows strain ellipses (derived from initial circles) and deformed grid (derived from initially square grid parallel to shear direction); profile on the left shows how the amount of shear γ varies across shear zone. Undeformed state (b) is mirror image of deformed state (a) and shows reciprocal strain ellipses. Strain trajectories in deformed state (c) and undeformed state (d) are one and the same material grid. Selected grid elements (stippled) show how trajectory curvatures change sign during deformation.

either family are non-parallel: they converge, forming fans. We refer to this geometry as a double fan, to distinguish it from the single fans described earlier. For a double fan, neither of the curvature equations in (1) vanish.

Mathematically or geometrically, a double fan can be generated by superposing two single fans, in such a way that the radial straight lines of the first fan become curved. Rather than follow this procedure, we prefer to describe three examples of geologically relevant strain fields containing double fans.

Example 5 (*Fig.* 5). *Shear zone*

In an ideal ductile shear zone, the deformation is a simple shear of varying amount γ. Values of γ reach a maximum in the center of the zone and fall symmetrically to zero at each margin. In both the deformed state (Fig. 5d) and its mirror image, the undeformed state (Fig. 5c), strain trajectories of each family curve into and out of the shear zone. Hence there are double fans at all points, except at the margins and along the middle line.

We now describe the geometry in more detail and use symmetry arguments to verify the curvature equations. Consider an element of length, ds, parallel to the shear direction in the deformed state. Elements of arc along the strain trajectories are then, by projection,

$$ds_1 = ds \cos \alpha; \quad ds_2 = ds \sin \alpha. \tag{8}$$

Similarly, in the undeformed state, a line element along the shear direction is dS, so that elements of arc along the strain trajectories are, by projection,

$$dS_1 = dS \cos A; \quad dS_2 = dS \sin A. \tag{9}$$

The main feature of simple shear is the invariant length of the shear direction:

$$ds = dS. \tag{10}$$

Also, because of mirror symmetry,

$$A + \alpha = 90°. \tag{11}$$

Using (10) and (11), equation (9) becomes:

$$dS_1 = ds \sin \alpha = ds_2; \quad dS_2 = ds \cos \alpha = ds_1. \tag{12}$$

Hence the principal stretches have the following values in terms of α (Cutler & Cobbold 1985):

$$\begin{aligned} \lambda_1 &= ds_1/dS_1 = ds_1/ds_2 = \cot \alpha \\ \lambda_2 &= ds_2/dS_2 = ds_2/ds_1 = \tan \alpha. \end{aligned} \tag{13}$$

The directional curvatures of the trajectories are

$$\begin{aligned} K_1 &= \partial A/\partial S_1 = -\partial \alpha/\partial s_2 = -k_2 \\ K_2 &= \partial A/\partial S_2 = -\partial \alpha/\partial s_1 = -k_1, \end{aligned} \tag{14}$$

where (10) and (11) have been used once again. Equation (14) can also be written down using symmetry.

From the foregoing equations, the flexures are easily calculated to be

$$f_1 = k_1/\sin^2 \alpha; \quad f_2 = k_2/\cos^2 \alpha. \tag{15}$$

If the strain trajectories were straight in the undeformed state, we would have $f_1 = k_1$ and $f_2 = k_2$ (as in example 1) and the convergence hypotheses would hold. Equation (15) shows that the convergence hypothesis also holds for a shear zone, but trajectory curvatures are less pronounced than in example 1, by factors of $\sin^2 \alpha$ and $\cos^2 \alpha$, respectively. Using (15), we can calculate the right-hand sides of the curvature equations (1):

$$\lambda_2(k_1 - f_1) = \tan \alpha(1 - \operatorname{cosec}^2 \alpha)k_1 = -k_1 \cot \alpha \tag{16a}$$

$$\lambda_1(k_2 - f_2) = \cot \alpha(1 - \sec^2 \alpha)k_2 \quad = -k_2 \tan \alpha, \tag{16b}$$

whereas the left-hand sides of the curvature equations are

$$\begin{aligned} K_1 &= -\partial \alpha/\partial s_2 = -\cot \alpha(\partial \alpha/\partial s_1) = -k_1 \cot \alpha \\ K_2 &= -\partial \alpha/\partial s_1 = -\tan \alpha(\partial \alpha/\partial s_2) = -k_2 \tan \alpha. \end{aligned} \tag{17}$$

The equivalence of (16) and (17) shows that the

curvature equations are verified. From (16a), we see that reversal of deformation causes the final directional curvature k_1 to be modified by the flexure f_1, to such an extent that the sense (sign) is reversed. Removal of the stretch λ_2 at the point in question then increases the true curvature, without further change of sign. The net result is that trajectory curvatures in either the deformed or the undeformed state are small compared with strain gradients f_1 and f_2. Thus the convergence hypothesis barely holds. Indeed the following example 6 shows that a small additional distortion suffices to change the signs of the directional curvatures, rendering the convergence hypothesis invalid.

Example 6 (*Fig.* 6). *Differential extrusion*

We first take a pattern of non-uniform simple shear, due to lateral symmetrical extrusion between two rough rigid vertical side-walls. Then we superimpose a small amount of simple flexure (as in example 1). This causes the side walls to become tilted out of parallelism (Fig. 6b). In the central part of the deformation field, λ_2 (λ_{max}) trajectories now converge strongly to the right (Fig. 6c); whereas strain intensity and λ_{max} values increase to the left (Fig. 6d); thus the convergence hypothesis does not hold. The explanation for this can be sought visually. Values of stretch λ_2 are between 1.1 and 1.3, but the flexure, $f_1 = -\partial\varepsilon_1/\partial s_2$, is significantly large in the deformed state; furthermore, original directional curvature K_1 (Fig. 6g) is greater in magnitude. These are almost the conditions for inverse flexure, (example 2) where the convergence hypothesis does not hold.

Near the left-hand corners of the extrusion field, trajectories have vanishingly small curvatures (Fig. 6c); yet there are strong stretch gradients along both families of trajectories. Thus in these corners the convergence hypothesis breaks down.

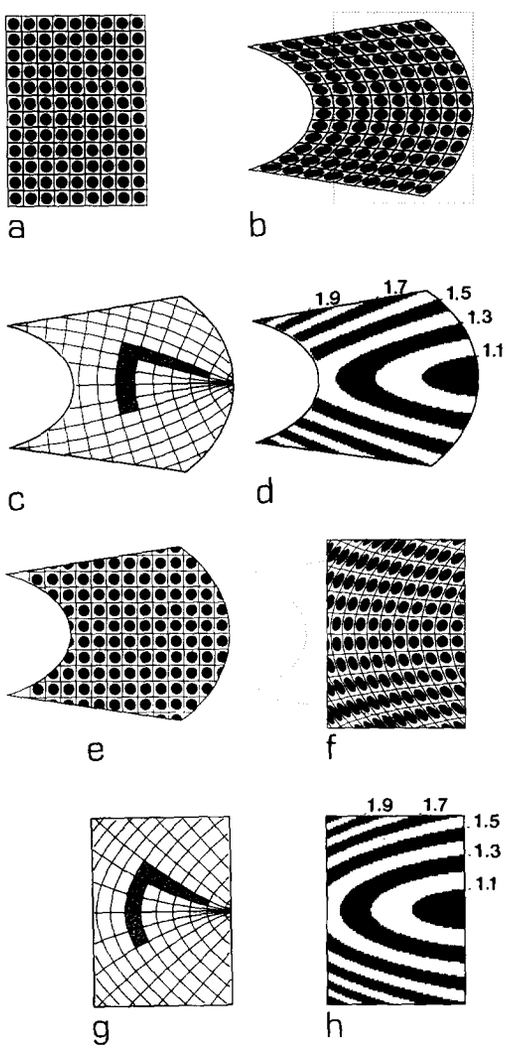

Fig. 6. Differential extrusion. Initially circular markers, within a square grid (a), become ellipses in deformed state (b). Strain trajectories (c) converge to the right in centre of region, but are more nearly straight and parallel in left-hand corners. Strain intensity (d), contoured for values of λ_2, decreases centrally and to the right. Reciprocal images (e)–(h) are for undeformed state. Strain trajectories in deformed state (c) and undeformed state (g) are one and the same material grid. Selected grid elements (stippled) show how radius of curvature changes with deformation.

Example 7 (*Fig.* 7). *Experimental diapirism*

To show that example 6 has mechanical and geological relevance, we reproduce an experimental result obtained by Dixon (1975). He modelled the buoyant uprise of a cylindrical ridge of silicone fluid, through a heavier fluid overburden, using silicone putties. A square grid was impressed upon a vertical section through the undeformed model. In the deformed state (Fig. 7a) the grid reveals displacements and allows strains to be calculated. We select two areas for discussion.

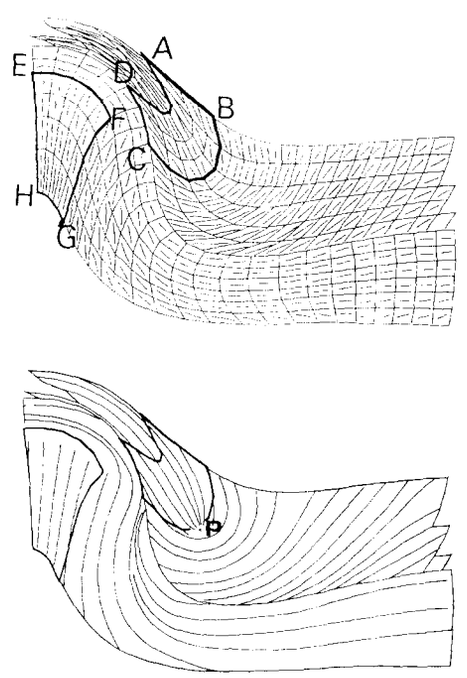

Fig. 7. Experimental diapirism (after Dixon 1975). Material grid (a), square before deformation, reveals displacements. Bars give orientations and approximate relative magnitudes of maximum stretches. Selected areas (ABCD and EFGH) are discussed in text. Strain trajectories (b) have been obtained numerically, by interpolation and integration.

The second area (EFGH, Fig. 7a) is near the centre of the rising dome. Here λ_{max} trajectories converge very gently downwards, whereas λ_{max} values increase strongly. The convergence hypothesis therefore holds, but only just.

In conclusion, this experimental example shows that the convergence hypothesis can hold in one area but not in another of the same strain field.

CONCLUSIONS

From our two-dimensional geometrical and mathematical study, we draw the following inescapable conclusions.

(1) Curvature of a strain trajectory in the deformed state depends upon three factors: (i) curvature in the undeformed state; (ii) magnitude of transverse stretch; and (iii) flexure (transverse gradient of trajectory-parallel logarithmic stretch).

(2) Depending upon the relative magnitudes of these three factors, so the convergence hypothesis may or may not hold.

(3) In the absence of other data, trajectory curvatures at a point in the deformed state are thus insufficient for geometric interpretation or strain removal.

(4) Stretch gradients may exist along parallel straight trajectories, even if there are no volume changes.

As the convergence hypothesis holds for ideal shear zones and simple fold models, and as strain patterns of these kinds are relatively common in nature, the geologist is entitled to wonder how reliable the hypothesis is as an empirical first approximation. Only a detailed assessment of field data and possibly mechanical analyses as well may one day provide an answer to this question. For the moment, we would advise caution in applying the convergence rule.

Acknowledgements—Aspects of this work were first presented by P. R. Cobbold at the University of California, Los Angeles, in 1983. Funding for his visit was shared by UCLA (Seminar program, Earth Sciences), NSF (award to W. D. Means) and CNRS (ATP US-France). G. Oertel arranged the visit. The introduction to this paper was totally rewritten as a result of useful comments by three referees (J. G. Ramsay, S. H. Treagus and anonymous).

REFERENCES

Borg, S. F. 1963. *Matrix-tensor Methods in Continuum Mechanics.* Van Nostrand, New Jersey.

Bourne, D. E. & Kendall, P. C. 1977. *Vector Analysis and Cartesian Tensors* (2nd Edn). Nelson, London.

Cobbold, P. R. 1977. Compatibility equations and the integration of finite strain in two dimensions. *Tectonophysics* **39**, T1–T6.

Cobbold, P. R. 1979. Removal of finite deformation using strain trajectories. *J. Struct. Geol.* **1**, 67–72.

Cobbold, P. R. 1980. Compatibility of two-dimensional strains and rotations along strain trajectories. *J. Struct. Geol.* **2**, 379–382.

Cobbold, P. R. & Percevault, M. N. 1983. Spatial integration of strains using finite elements. *J. Struct. Geol.* **5**, 299–305.

Cutler, J. M. & Cobbold, P. R. 1985. A geometric approach to two-dimensional finite strain compatibility: interpretation and review. *J. Struct. Geol.* **7**, 727–736.

De Paor, D. G. 1983. Orthographic analysis of geological structures—I. Deformation theory. *J. Struct. Geol.* **5**, 255–277.

Dixon, J. M. 1975. Finite strain and progressive deformation in models of diapiric structures. *Tectonophysics* **28**, 89–124.

Ramsay, J. G. 1967. *Folding and Fracturing of Rocks.* McGraw-Hill, New York.

Ramsay, J. G. & Graham, R. H. 1970. Strain-variation in shear-belts. *Can. J. Earth Sci.* **7**, 786–813.

Ramsay, J. G. & Huber, M. I. 1983. *The Techniques of Modern Structural Geology. Vol. 1, Strain Analysis.* Academic Press, London.

Ramsay, J. G. & Huber, M. I. 1987. *The Techniques of Modern Structural Geology. Vol. 2. Folds and Fractures.* Academic Press, London.

Schwerdtner, W. M. 1977. Geometric interpretation of regional strain analyses. *Tectonophysics* **39**, 515–531.

Siddans, A. W. B. 1972. Slaty cleavage—a review of research since 1815. *Earth Sci. Rev.* **8**, 205–232.

Signorini, A. 1943. Transformazioni termoelastiche finite. *Memoria la, Annali di Matematica*, serie IV, Tomo XXII, 33–143.

Truesdell, C. & Toupin, R. 1960. The classical field theories. In: *Handbüch der Physik* (edited by Flügge, S.), Vol. 3. Springer-Verlag, Berlin, 226–793.

Williams, P. F. 1976. Relationships between axial-plane foliations and strain. *Tectonophysics* **30**, 181–196.

Wood, D. S. 1974. Current views of the development of slaty cleavage. *Ann. Rev. Earth Planet. Sci.* **2**, 369–401.

APPENDIX

DERIVATION OF CURVATURE EQUATIONS

We derive curvature equations for strain trajectories, starting from first principles. The equations are in fact simple forms of compatibility conditions for strains. The standard mathematical way of deriving and expressing such compatibility conditions is via the Riemann–Christoffel curvature tensor, $\boldsymbol{R}$ (Truesdell & Toupin 1960, p. 272). In general, this curvature tensor is defined in terms of a metric tensor. If the metric tensor is chosen to be Cauchy's strain tensor, $\boldsymbol{c}$, then the compatibility amongst the components of $\boldsymbol{c}$ leads to $\boldsymbol{R} = 0$. Thus the vanishing of $\boldsymbol{R}$ is perhaps the simplest and most elegant mathematical way of expressing strain compatibility; but it is also difficult to understand in detail and difficult to interpret geometrically.

An alternative and more explicit approach was used by Signorini (1943) to express compatibility amongst strains and rotations. The method was rediscovered in a geological context by Cobbold (1977, 1980) and reviewed by Cutler & Cobbold (1985). Here we start once again from first principles, but take the method a little further, so as to obtain simple curvature equations.

Consider a smooth grid of orthogonal curvilinear co-ordinates, x_1 and x_2, parallel to strain trajectories in the deformed state. The exact shape of this grid we suppose to be defined by the co-ordinate transformation

$$x_1 = x_1(z_1, z_2); \quad x_2 = x_2(z_1, z_2), \tag{A1}$$

where z_1 and z_2 are common Cartesian co-ordinates. Elements of both grids are linearly related, as follows:

$$\begin{bmatrix} dz_1 \\ dz_2 \end{bmatrix} = \begin{bmatrix} \partial z_1/\partial x_1 & \partial z_1/\partial x_2 \\ \partial z_2/\partial x_1 & \partial z_2/\partial x_2 \end{bmatrix} \begin{bmatrix} dx_1 \\ dx_2 \end{bmatrix}. \tag{A2}$$

where the matrix on the right contains the components of the transformation gradient tensor. Because the curvilinear co-ordinates x_1 and x_2 are orthogonal, the transformation gradient can be expressed as the product of (i) a rigid rotation through an angle α (positive if anticlockwise from z_1) and (ii) a shape change with scale factors h_1 and h_2:

$$\begin{bmatrix} \partial z_1/\partial x_1 & \partial z_1/\partial x_2 \\ \partial z_2/\partial x_1 & \partial z_2/\partial x_2 \end{bmatrix} = \begin{bmatrix} \cos\alpha & \sin\alpha \\ -\sin\alpha & \cos\alpha \end{bmatrix} \begin{bmatrix} h_1 & 0 \\ 0 & h_2 \end{bmatrix}. \tag{A3}$$

Now h_1 and h_2 cannot vary in space independently of each other, because the components of the transformation gradient tensor must satisfy the following compatibility equations:

$$\frac{\partial}{\partial x_2}\left(\frac{\partial z_1}{\partial x_1}\right) = \frac{\partial}{\partial x_1}\left(\frac{\partial z_1}{\partial x_2}\right); \quad \frac{\partial}{\partial x_2}\left(\frac{\partial z_2}{\partial x_1}\right) \frac{\partial}{\partial x_1}\left(\frac{\partial z_2}{\partial x_2}\right). \tag{A4}$$

Substitution of (A3) into (A4) yields, after some algebra,

$$\partial\alpha/\partial x_1 = (-1/h_2)\,\partial h_1/\partial x_2; \quad \partial\alpha/\partial x_2 = (1/h_1)\,\partial h_2/\partial x_1. \tag{A5}$$

Equations (A1)–(A5) are identical to those of Cobbold (1980,

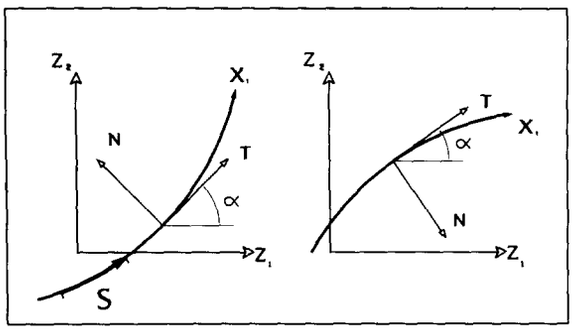

Fig. A1. Curvature and directional curvature of a strain trajectory. $\boldsymbol{T}$ is a unit vector tangent to trajectory. $\boldsymbol{N}$ is a unit vector normal to trajectory and pointing towards centre of curvature, i.e. top left (a) or bottom right (b). True curvatures are identical in both examples, but directional curvatures are of opposite sign. See text for details and references.

equations 1–5). Those of Cutler & Cobbold (1985, equations 1, 2, 3, 8 and 11) differ only in that they represent the undeformed state and hence are written in upper-case letters. Equations (A5) express grid curvature (left) and its alternative definition in terms of grid spacing (right). More familiar measures of curvature are obtained by considering elements of true distance along the x_1 and x_2 directions:

$$ds_1 = h_1\,dx_1; \quad ds_2 = h_2\,dx_2, \tag{A6}$$

where s_1 and s_2 are true arc lengths, not co-ordinates. Substituting (A6) into (A5), we obtain the linear relationships (see Cobbold 1980)

$$k_1 = \partial\alpha/\partial s_1 = -\partial b_1/\partial s_2; \quad k_2 = \partial\alpha/\partial s_2 = \partial b_2/\partial s_1, \tag{A7}$$

where b_1 and b_2 are logarithmic scale factors given by

$$b_1 = \ln h_1; \quad b_2 = \ln h_2. \tag{A8}$$

The quantities k_1 and k_2 in (A7) are measures of curvature. The usual way of defining the curvature of a line at a point P (see, for example, Bourne & Kendall 1977, p. 63) is first to define a unit vector, $\boldsymbol{T}$, tangent to the curve at P (Fig. A1). The rate of change of $\boldsymbol{T}$ with positive distance s along the curve, is $d\boldsymbol{T}/ds$. This quantity is equal to $\varkappa\boldsymbol{N}$, where $\boldsymbol{N}$ is a unit vector normal to the curve at P, and $\varkappa$ is a positive scalar quantity, known as the curvature. In two dimensions $\varkappa$ is the absolute value of the quantity $k = \partial\alpha/\partial s$ used in equation (A7) above (Bourne & Kendall 1977, p. 66). In fact, k can be positive or negative, depending upon the direction of the unit normal, $\boldsymbol{N}$ (Fig. A1). Thus we refer to k as the directional curvature. The radius of curvature is defined as $r = 1/\varkappa = 1/|k|$.

Strain trajectories in the undeformed state can be represented in a similar way, using another set of orthogonal curvilinear co-ordinates. We denote these as X_1 and X_2 and refer them to a Cartesian frame Z_1, Z_2. Hence, using upper-case letters instead of their lower-case equivalents, equations (A1)–(A8) may be rewritten and become valid for the undeformed state. In particular, equations (7) become

$$K_1 = \partial A/\partial S_1 = -\partial B_1/\partial S_2$$
$$K_2 = \partial A/\partial S_2 = \partial B_2/\partial S_1. \tag{A9}$$

As a result of deformation, strain trajectories in the undeformed state become strain trajectories in the deformed state (Cobbold 1979). For convenience, we may assume that X_1 and X_2 become x_1 and x_2, respectively, so that deformation is simply expressed as

$$x_1 = X_1; \quad x_2 = X_2. \tag{A10}$$

The reader can easily check that equation (A3), together with its equivalent in upper-case letters for the undeformed state, when both substituted into (10), yield the usual relationship between Cartesian frames $\boldsymbol{z}$ and $\boldsymbol{Z}$ (e.g. De Paor 1983, equation 78):

$$\begin{bmatrix} \partial z_1/\partial Z_1 & \partial z_1/\partial Z_2 \\ \partial z_2/\partial Z_1 & \partial z_2/\partial Z_2 \end{bmatrix} = \begin{bmatrix} \cos\alpha & -\sin\alpha \\ \sin\alpha & \cos\alpha \end{bmatrix} \begin{bmatrix} \lambda_1 & 0 \\ 0 & \lambda_2 \end{bmatrix} \begin{bmatrix} \cos A & \sin A \\ -\sin A & \cos A \end{bmatrix}, \tag{A11}$$

where λ_1 and λ_2, the principal stretches in the nomenclature of Truesdell & Toupin (1960), are given by

$$\lambda_1 = h_1/H_1; \quad \lambda_2 = h_2/H_2. \tag{A12}$$

Taking logarithms of both sides of (A12), we define the logarithmic stretches:

$$\varepsilon_1 = \ln\lambda_1 = b_1 - B_1; \quad \varepsilon_2 = \ln\lambda_2 = b_2 - B_2, \tag{A13}$$

where (A8) and its upper-case equivalent have been used.

Now we are in a position to investigate how the directional curvatures change as a result of deformation. We substitute (A12) and (A13) and the upper-case equivalent of (A6) into (A9); then we compare the result with (A7). This yields the required expressions for curvature change:

$$K_1 = \lambda_2(k_1 - f_1); \quad K_2 = \lambda_1(k_2 - f_2), \tag{A14}$$

where f_1 and f_2 we define to be the *flexures*, in other words the strain gradients

$$f_1 = -\partial\varepsilon_1/\partial s_2; \quad f_2 = \partial\varepsilon_2/\partial s_1. \tag{A15}$$

There is a clear mathematical analogy between the flexures defined in (A15) and the directional curvatures defined in (A7).

Three-dimensional equivalents of the above 2-D equations can be derived in the same way (see Borg 1963, pp. 75–76, for a partial discussion), but require more careful definition of curvatures and rotations. We leave the topic to a future publication.